POLITECNICO DI TORINO
Repository ISTITUZIONALE

CFD optimization of large water storages for efficient cooling of high power intermittent thermal loads

(Article begins on next page)
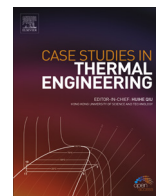
26 April 2024

CFD optimization of large water storages for efficient cooling of high power intermittent thermal loads

Marco Simonetti*, Vincenzo Maria Gentile

DENERG Department of Energy, Politecnico di Torino, c.so Duca degli Abruzzi 24, 10129, Torino, Italy

ARTICLE INFO

ABSTRACT

The design optimization of water basins for the refrigeration of intermittent high-power heat sources, by mean of CFD simulations, is presented. A case study of an experimental facility is considered, that foreseen two large water basins as thermal storage, with volume of 315 m^3 and 500 m^3 respectively, and an installed nominal cooling power around 25 MW for the cooling of an intermittent load, with peak power of around 65 MW. A strong horizontal stratification has been looked after in the preliminary design, which include a labyrinth of walls and weirs, and water inlet/outlet plugs positioned at the opposite side of the basins. The intensity and the role of this stratification have been explored using a CFD software, simulating both winter and summer sceneries. Some variants to the original design have been studied, in order to optimize the stratification of water temperatures. It is shown that a large water storage with an optimal design could help very much in reducing cooling power demand in case of intermittent thermal load.

1. Introduction

This paper describes the optimization of two large water basins, used as cooling energy storages for the refrigeration of inter-mittent high-power sources. Sources of this kind can be found in industrial applications and in specific experimental test facilities. In the case study presented here, the water basins are cooled by dry coolers and by evaporative towers. Hence, cooling power to the storages are weather-sensitive, and a winter and a summer scenario are depicted. The total installed nominal cooling power is 25 MW, during winter time. Thermal load peak power is around 65 MW, with intermittent operative profile. Large storages were preliminarily designed with a lumped parameter model, in order to reduce the installed cooling power to a fraction of this load.

Reserving cool thermal energy for peak-shaving operation is not a new concept. Recently, more attention has been given to PCM (Phase Change Materials), while in the past the largest number of applications considered ice storage. Ice storage applications are commonly considered for shifting the electricity consumption into a more convenient tariff time of the day. Adding little water storages in the refrigeration systems is a widely-applied design rule in order to avoid intermittent operation of the compressors of chillers. However, in this case, the sizing of the chillers is normally set to meet the full peak power load. Large water storage has been less considered, because it represents a lower energy-density system [1]. Nonetheless, water storage has been seldom chosen for peak shavings in case of large systems [2,3].

In the past, some works have been devoted to chilled water tank stratification. In fact, water mixing in a tank is responsible of a lower storage efficiency, either considering a 1st law and a 2nd law approach [4,5]. In order to improve temperature stratification, and to limit the water mixing, the vertical configuration has been more often investigated, in which natural buoyancy is fostered [6–9].
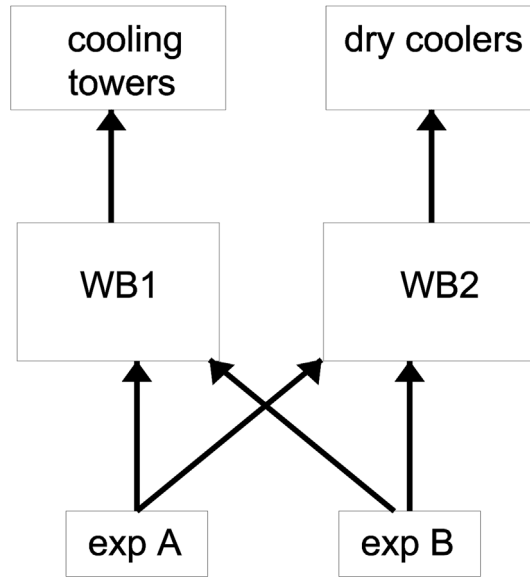

Fig. 1. Blocks scheme of the facility.

Horizontal stratification has been seldom studied [10,11]. In order to increase thermal stratification, plates [12] or labyrinth [11] have been studied and applied.

In the preliminary design of the storages described in this work, a labyrinth of walls and weirs was designed in the basins, to achieve and keep a relevant horizontal temperature stratification.

3D transient CFD simulation is a powerful instrument for the analysis of complex storage system, even if it may be not universally adopted for its complexity, as the water storage gets larger [13]. However, it is especially useful in case of 3D effects that cannot be covered in details by 1D and 2D simplified analytical methods [14], which in the vast majority focus on natural thermocline in vertical gradient and do not consider complex labyrinths.

In this work, by mean of CFD simulations, the transient operative scenarios in winter and summer have been studied and optimized.

2. Case study description

In the case study, 2 high power physics experiments need to be cooled by the system.

The two experiments are cooled by mean of a cooling plant, composed by 2 large water basins (WB), storing chilled water. One basin (WB1) is of 315 m^3 volume and the second (WB2) of 545 m^3.

The two basins are served, respectively, by a set of evaporative towers and by a set of dry coolers (Fig. 1).

Design conditions for these systems are reported in Table 1 and Table 2.

The two experiments, A and B, are used in two modes, with intermittent operational profiles, mode 1 and mode 2. In mode 1, only experiment A operates with the following cycle: 1 h (3′600 s) full power, 3 h recover. Full cooling power needs of experiment A is 59 MW.

In mode 2, experiments A and B are operated, with the following duty cycle: 300 s power on, 900 s power off. Experiment A power is the same of mode A, i.e. 59 MW, while experiment B adds around 10.5 MW of cooling load.

The thermal power (cooling load) deployed in the two operative modes are shared by the storages, following the description of Table 3.

Mode 1 is used in winter average time only, while mode 2 is activated during summer, as long as the chilled water available from the storage to the experiments is below the operative limit of 50 °C. Reference outdoor conditions are reported in Table 4.

Table 1
Design conditions for cooling towers, serving WB1.

Cooling power [kW]	Temperature of the water inlet [°C]	Outdoor wet bulb air temperature [°C]
2′880	15	8
6′000	18	8
15′600	30	8
16′801	44	26

Table 2

Design conditions for dry cooler, serving WB2.

Cooling power [kW]	Temperature of water inlet [°C]	Outdoor dry bulb air temperature [°C]
17′373	36	10
25′647	72	34

Table 3

Power shares of the storages in the two operative modes.

Operative mode	Power to WB1 [MW]	Power to WB2 [MW]
mode 1 - winter	16	43
mode 2 - summer	20	52

Table 4

Reference outdoor condition for calculation.

Season	External air temperature dry bulb [°C]	External air temperature wet bulb [°C]	Relative humidity
winter	10	8	80%
summer	34	26	50%

3. CFD models description

3.1. a. Geometries

The aim of this study is to find an optimal configuration of the cooling basins. Three different configurations have been studied:

Configuration A: the basin is provided with a labyrinth composed by a regular array of walls and weirs. Water flows aside of the walls, which present the free area for water passage alternatively on different side, while weirs have it on top (Fig. 2). The same module is repeated along WB1 and WB2.

Configuration B: the number of walls and weirs in the basin is increased by a factor 2, resulting in a more articulated path for the water flow;

Configuration C: the positions of the free passage area in the wall is varied compared to case A. The upper wide horizontal water flow areas of the weirs are moved to the bottom part of the walls, leaving unchanged the lateral passage areas of the walls.

Experiments to be cooled are supplied from the outlets located on the right side of the basin; the return flow enters into the basin in the left side. The cooling system operates in the central part of the basin (Fig. 3).

Water basin 1 (WB1) and water basin 2 (WB2) share a similar design.

All the configurations have been meshed with polyhedral cells. In this particular application, wall heat transfers play a marginal role, hence the mesh at wall boundaries can be kept coarse enough to allow a time-effective transient simulation with a standard work-station (in this work a quad-core processor with 32 Gbytes RAM is used).

A grid independence test has been performed ad a mesh of 791′490 cells have been selected for WB1, and 1′204′500 for WB2.
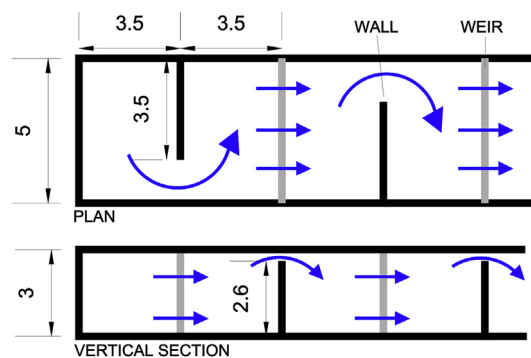

Fig. 2. Module of the labyrinth of walls and weirs in the two water basins. Length unit [m].
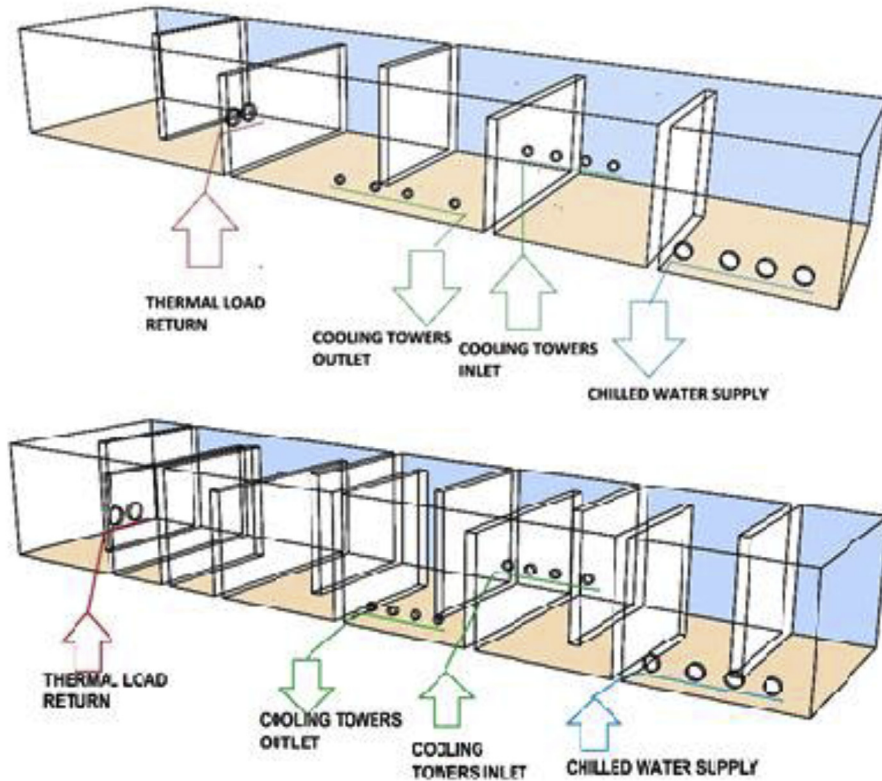
Fig. 3. Up: Water basins configuration A (WB1-A); Down: Water basin configuration B, with number of walls and weirs increased by factor 2 (WB1–B).

3.2. b. Modelling options

In the following Table 5, the main modelling option and boundary conditions are recalled.

3.3. c. Operative conditions

Three non-dimensional numbers can be considered in order to characterize the water flow in the basins.
Reynolds number (*Re*) is calculated as:

$$Re = \frac{\bar{U}L}{\nu}$$

(1)

Table 5
Modelling input for CFD.

Category	Name	Input
Modelling options	Solver	Transient segregated
	Pressure-velocity coupling	SIMPLE
	Spatial discretization pressure	Body Force Weighted
	Spatial discretization momentum	QUICK
	Buoyancy modelling	Boussinesq
	Turbulence modelling	κ-ω
Boundary conditions	Walls bottom and verticals walls	Adiabatic
	Top wall	Adiabatic. No friction (in order to simulate a flat free surface of water)
	Thermal load circuit inlet	WB1: 341 kg/s constant mass flow rate. Variable temperature. Turbulence intensity 10%
		WB2: 291 kg/s constant mass flow rate. Variable temperature. Turbulence intensity 10%
	Cooling circuit inlet	WB1: 301 kg/s constant mass flow rate. Variable temperature. Turbulence intensity 10%
		WB2: 438 kg/s constant mass flow rate. Variable temperature. Turbulence intensity 10%
Initial conditions	Water basin temperature	18 °C
	Water velocity in the basin	0 m/s

where:

$$\bar{U} = average\ water\ velocity\ \left[\frac{m}{s}\right] = \frac{\dot{V}}{A} = \frac{volumetric\ flow\ rate\ \left[\frac{m^3}{s}\right]}{basin\ transversal\ area\ [m^2]}$$

$$L = characteristic\ lenght = equivalent\ diameter = \frac{4A}{2p} = \frac{4\ basin\ transversal\ area\ [m^2]}{basin\ transversal\ perimeter\ [m]}$$

$$\nu = water\ cinematic\ viscosity\ \left[\frac{m^2}{s}\right]$$

the Grashof number (*Gr*), is calculated as:

$$Gr = \frac{gL^3\beta(T_J - T_i)}{\nu^2} \tag{2}$$

where:

g = gravity acceleration [m/s^s]
β = coefficient of thermal expansion [1/K]
T_J = temperature of the inlet jet [˚C]
T_i = initial temperature of the water basin [˚C]

and the Richardson number (*Ri*) is calculated as:

$$Ri = \frac{Gr}{Re^2} \tag{3}$$

In the following (Table 6) the average values of the three numbers are exposed, calculated considering reference average values of the initial conditions.

The Richardson number, representing the ratio of buoyancy to inertia forces in the storage tank, has been widely used to measure stratification. Storage tanks with higher *Ri* experience greater stratification because the momentum of the incoming fluid stream is insufficient to overcome the temperature difference induced buoyancy forces, leading to reduced mixing of the inlet stream with the resident fluid, and causing the inlet fluid emersion to the top of the storage tank.

4. Design optimization

4.1. a. Winter scenario optimization

Three configurations, A,B and C, described in par.3.1, are considered for the optimization. These variations tend to increase the horizontal and vertical stratification effect in the basins. A higher stratification represents an improvement in term of a lower temperature of the cooling water supplied to the experiment. Conversely, it could produce a longer recharge time of the storage.

WB1 is studied in mode 1; the following figures show contours of water temperatures at the walls of the basins at time 3600 s (end of the long pulse) (Fig. 4).

Table 7 shows the temporal evolution of temperatures of water cooling to experiment and mean temperature of water basins, for three different configurations A, B and C.

Table 7 results do confirm that the labyrinth is effective in avoiding the quick mixing of the water in the basins.

Configuration B, with doubled number of walls, performs better then configuration A. Configuration C is the best performer.

It can be seen that configuration C, with bottom water passages in the weirs, gives a significant advantage in term of temperature of the water to the experiments. It can be appreciated from Fig. 5 that the configuration C fosters the vertical positive gradient of temperature, due to buoyancy and high *Ri* number (Table 6).

Table 6
Characteristic operative values.

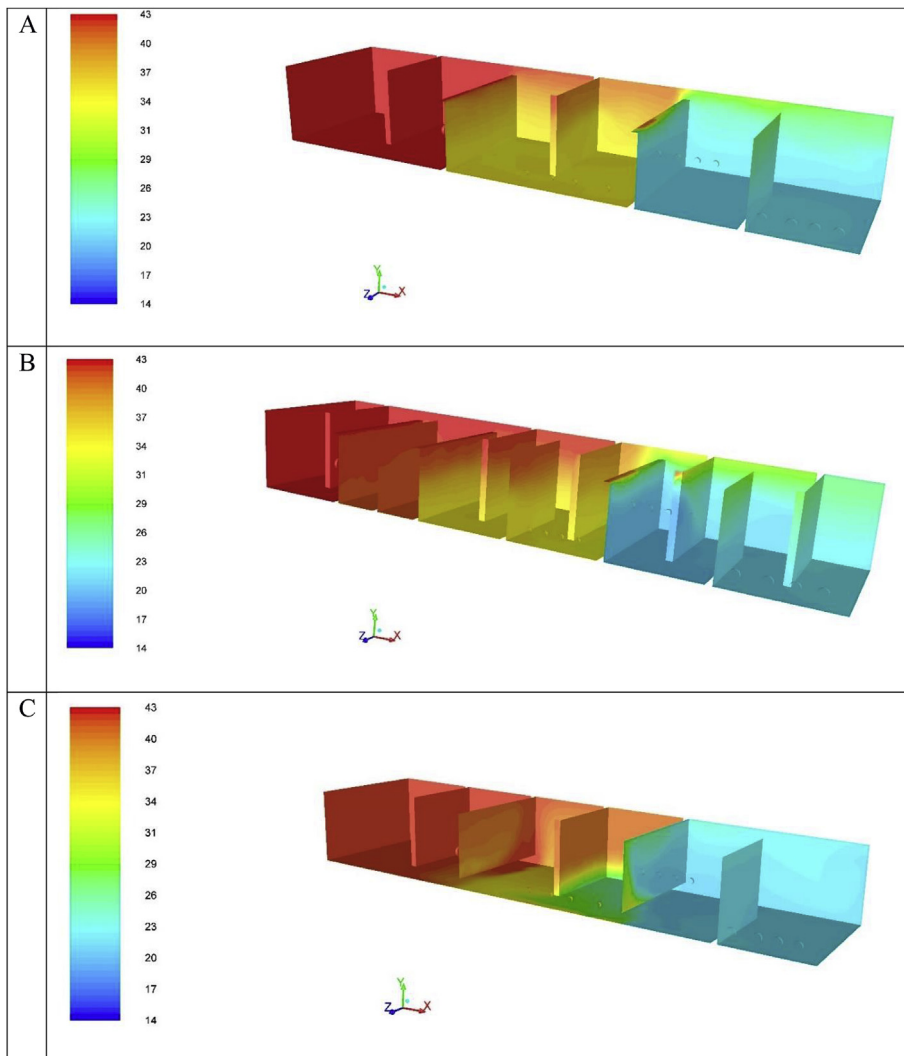|	WB1		WB2		units
	Cooling	Recharge	Cooling	Recharge	
avrg U	0.023	0.02	0.019	0.029	*m/s*
Re	131′154	116′154	111′923	168′462	-
T_j	53	18	62	35	*˚C*
T_i	18	35	20	45	*˚C*
Gr	4.29E + 16	2.08E + 16	5.14E + 16	1.22E + 16	-
Ri	2′491′392	1′542′829	4′105′311	431′454	-

Fig. 4. WB1-configuration A, B, C, mode 1, time 3′600 s (end of pulse), contour of water temperature at wall [°C].

Table 7
Mean basin water temperature and cooling water temperature temporal evolution for different configurations, in operation mode.

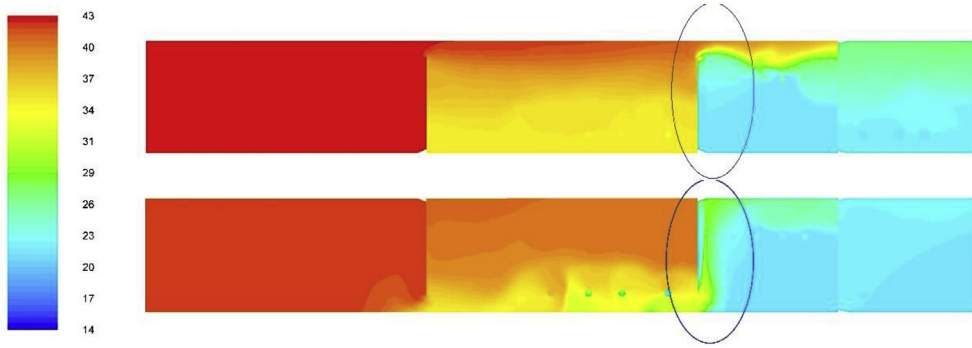| time [s]	mean water temperature [°C]	cooling water supply to the experiment temp. [°C]
WB1 configuration A		
800	25,7	17,7
1800	31,5	21,0
2800	33,9	22,0
3600	34,6	22,1
WB1 configuration B		
800	25,7	18,1
1800	30,8	20,4
2800	33,4	21,6
3600	34,4	21,9
WB 1 configuration C		
800	25,8	15,8
1800	31,1	18,6
2800	33,4	20,7
3600	34,3	21,4

Fig. 5. WB1 configuration A (top) and C (bottom) – mode 1, time 3'600 s (end of pulse) – contours of temperature on longitudinal vertical section [°C].

A drawback of this improvement is that during the recharge phase in mode 1 (winter) a significant vertical temperature gradient establishes in the middle section of the basin. In order to have a better delta of temperature on the cooling tower, it looks promising to introduce a secondary intake for cooling tower circuit, positioned on a higher level than the original one. This secondary intake, or outlet, could be conveniently used during recharge phase only.

The variation produces a more effective re-cooling (recharge) phase in the basin. The average temperature in the basin, at the end of the recharge phase, is around 1 °C lower for configuration C2. Hence, this final design is adopted for the complete set of simulation.

5. Optimized configuration results and comments

5.1. a. Mode 1 - winter

The trends of temperature during the operating phase of the experiment for WB1 are shown in Fig. 6, from which it can be commented that:

- during the operating phase of the experiment, the experiment is cooled by a water flow at a temperature of about 8 °C lower than the average temperature of the basin;
- when the experiment stops the horizontal thermal stratification is characterized by a temperature difference of 15 °C, corresponding to an average horizontal thermal gradient of 0.7 °C/m;
- through the thermal stratification of the basin it is possible to feed the experiment at a temperature close to the temperature of the cooling towers backflow.

The supply temperature of the experiment decreases during the first minutes of operation because the cooling system cools the water down to a temperature lower than the initial conservative guess. During this system warming up, the experiment backflow (yellow dotted line) temperature peaks to nearly 34 °C, and reduces after, as soon as the experiment supply (light blue dotted) reduces.
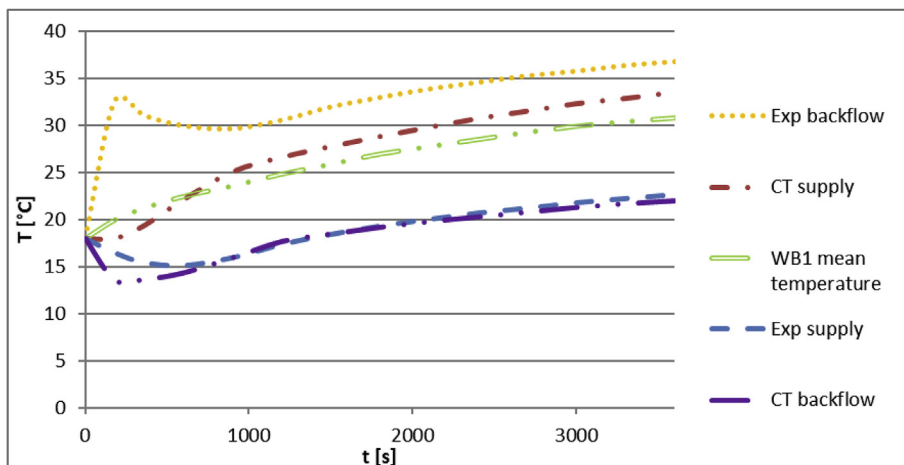

Fig. 6. WB1–C2, mode 1 (winter) temperature evolution (CT = Cooling Tower, Exp = experiment).
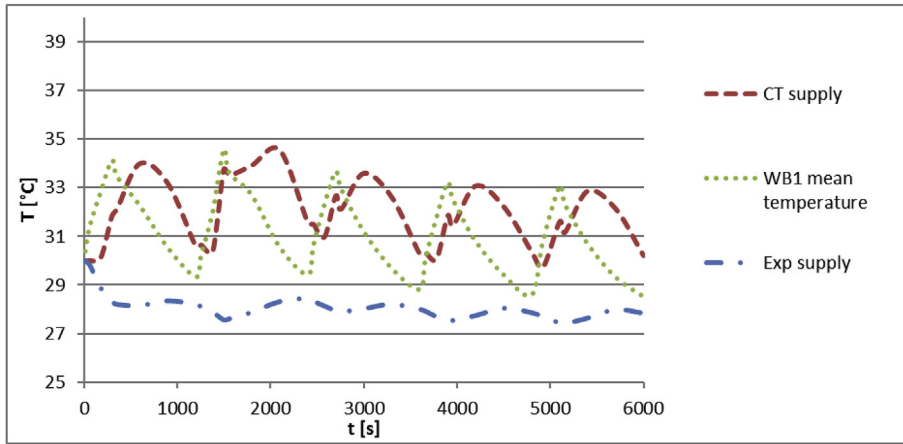
Fig. 7. WB1–C2, mode 2 (summer) temperature evolution (CT= Cooling Tower, Exp = experiment).

After the 3′600 s pulse, a recharge phase follows. In order to increase the cooling effectiveness, the water circuit of the experiment is by-passed and used in a recirculation mode. At the end of the recharge phase, where the average temperature is close to the initial value of 18 °C, the stratification of the basin is reduced to 5 °C. This corresponds to the delta of temperature CT supply - CT backflow.

WB2 performance is very similar to the WB1 for winter operation.

5.2. b. Mode 2 – summer

During operative mode 2, in summer condition, the WB1 basin operates under dynamically stable performance. Even if an average temperature of the basin follows a 5 °C swinging behaviour, the supply temperature to the experiment is almost steady and varying around 28 °C (see Fig. 7).

WB2, however, shows a more critical behaviour. WB2 is served by dry air-coolers, while WB1 is served by evaporative coolers, somehow more effective. WB2 is designed for a limit operative temperature of 55 °C. During the preliminary design phase a lumped parameter modelwas developed, where all the water in the basing was considered to be at uniform temperature and all the heat transfers to be a function of this singular temperature. In that study a limit to the number of pulses from the experiment, before WB2 reaches 55 °C, was identified. 5 pulses were considered as the maximum number of operative cycles before the storage needs a longer recharge.

The 3D CFD foresees a more effective performance of the basin than lumped parameter did. This is due to two positive effects of the capacity of modelling the thermal horizontal stratification. The first is that the cooling water supply is not at the average temperature of the basin, due to the stratification, so it eventually reaches the maximum temperature limit later than the average temperature. The second is that the water taken from the basin and sent to the air cooler (AC) is, conversely, at a higher temperature than the average, due the same stratification phenomena. This implies that the air coolers are performing at a higher temperature approach than the one foreseen by the lumped parameter model. Hence, they are actually rejecting more heat and operating at higher
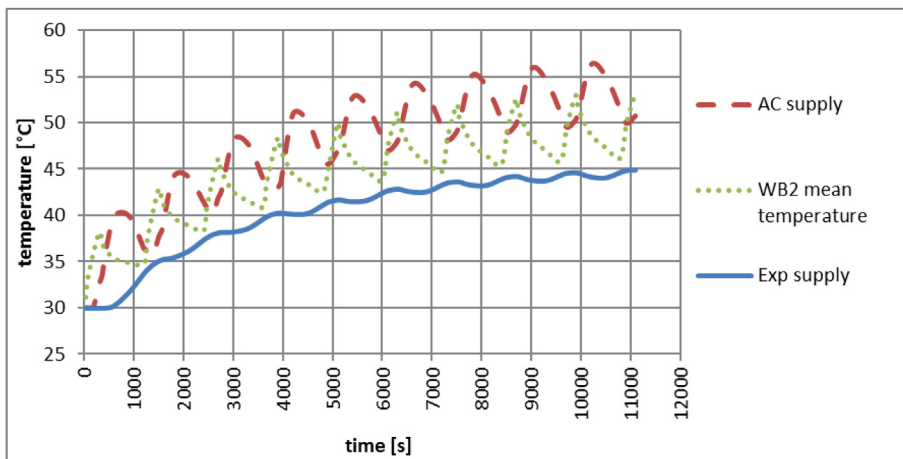
Fig. 8. WB2–C2, mode 2 (summer) temperature evolution (AC = Air Cooler, Exp = experiment).

cooling power. This fact explains why in Fig. 8 not only the cooling supply temperature to the experiments never reaches the maximum temperature limit, but even the average temperature calculated by the CFD is, after 9 pulses, above this limit.

6. Conclusions

The CFD is a powerful instrument for the optimization of large water storages designed for the cooling of high power intermittent loads. Study on large water basins are not common in literature. The here presented design of large basins, provided with labyrinth of walls and weirs, demonstrated a good effectiveness in achieving a positive temperature stratification. An average horizontal temperature gradient of 0.7 °C/m has been calculated.

It is shown that weirs with bottom flow area are more effective in increasing horizontal stratification then the ones with upper holes. In fact, in such large basins the Richardson number is high, and the vertical buoyancy effects dominate the flow. In this scenario, vertical gradient can be conveniently fostered by filtering the lower, cooler, part of the water flow by mean of the optimized weirs. Conversely, a dense and stratification-keeper labyrinth is a limit to the efficiency of the recharging of the storage. Especially in the case of intermittent loads, as in this study, a good balance of these opposite behaviors must be achieved.

The optimized design of the large water storages allowed the cooling of around 65 MW intermittent loads by installing only air-coolers and wet cooling towers, for a nominal power of less than 25 MW.

Acknowledges

References

[1] A.V. Novo, J.R. Bayon, D. Castro-Fresno, J. Rodriguez-Hernandez, Review of seasonal heat storage in large basins: water tanks and gravel-water pits, Appl. Energy 87 (2) (2010) 390–397.
[2] S. Boonnasa, P. Namprakai, The chilled water storage analysis for a university building cooling system, Appl. Therm. Eng. 30 (11–12) (2010) 1396–1408.
[3] G.P. Henze, B. Biffar, D. Kohn, M.P. Becker, Optimal design and operation of a thermal storage system for a chilled water plant serving pharmaceutical buildings, Energy Build. 40 (6) (2008) 1004–1019.
[4] M.Y. Haller, C.A. Cruickshank, W. Streicher, S.J. Harrison, E. Andersen, S. Furbo, Methods to determine stratification efficiency of thermal energy storage processes - review and theoretical comparison, Sol. Energy 83 (10) (2009) 1847–1860.
[5] P. Pinel, C.A. Cruickshank, I. Beausoleil-Morrison, A. Wills, A review of available methods for seasonal storage of solar thermal energy in residential applications, Renew. Sustain. Energy Rev. 15 (7) (2011) 3341–3359.
[6] Y.M. Han, R.Z. Wang, Y.J. Dai, Thermal stratification within the water tank, Renew. Sustain. Energy Rev. 13 (5) (2009) 1014–1026.
[7] S.M. Hasnain, Review on sustainable thermal energy storage technologies, Part II: cool thermal storage, Energy Convers. Manag. 39 (11) (1998) 1139–1153.
[8] M.A. Karim, Experimental investigation of a stratified chilled-water thermal storage system, Appl. Therm. Eng. 31 (11–12) (2011) 1853–1860.
[9] J.E.B. Nelson, A.R. Balakrishnan, S. Srinivasa Murthy, Parametric studies on thermally stratified chilled water storage systems, Appl. Therm. Eng. 19 (1) (1999) 89–115.
[10] S. Alizadeh, An experimental and numerical study of thermal stratification in a horizontal cylindrical solar storage tank, Sol. Energy 66 (6) (1999) 409–421.
[11] I. Dincer, M.A. Rosen, *Heat Storage Systems,* in *Exergy Analysis Of Heating, Refrigerating And Air Conditioning*, Elsevier, 2015, pp. 221–278, https://doi.org/10.1016/B978-0-12-417203-6.00006-5.
[12] A. Zachar, I. Farkas, F. Szlivka, Numerical analyses of the impact of plates for thermal stratification inside a storage tank with upper and lower inlet flows, Sol. Energy 74 (4) (2003) 287–302.
[13] A. Pizzolato, F. Donato, V. Verda, M. Santarelli, CFD-based reduced model for the simulation of thermocline thermal energy storage systems, Appl. Therm. Eng. 76 (2015) 391–399.
[14] H.O. Njoku, O.V. Ekechukwu, S.O. Onyegegbu, Analysis of stratified thermal storage systems: an overview, Heat Mass Transf. 50 (2014) 1017–1030.